

Dynamics of Isoconcentration Surfaces in Weak Shock Turbulent Mixing Interaction

L. Vervisch* and J. Réveillon†

Institut National des Sciences Appliquées de Rouen, Mont-St-Aignan 76821, France

When developing closures for nonpremixed turbulent combustion occurring in supersonic regime, the probability density function is an attractive approach. It is required, however, to find an appropriate strategy to close the diffusive (mixing) part of the problem. Within supersonic turbulent combustion devices, mixing layers interact with shock waves and compression zones. Hence, it is crucial to seek out basic effects related to pressure jumps needing to be accounted for in modeling mixing. Direct numerical simulations are performed to investigate properties of mixing in weakly nonisentropic flows. The simulations correspond to the interaction between a weak shock and a mixing zone. Different conditions for injecting the mixing zone upstream from the weak shock are considered in the simulations. First, it is observed that the appearance of secondary pressure waves attached to the weak shock can be justified in the light of previous studies devoted to shock vortex interactions. Results suggest that the hypothesis of a linear relationship between the frequency of mixing and the inverse of an eddy breakup time fails within the interaction zone. Then, a statistical formalism, suitable to describe isoconcentration surfaces, is chosen to study increase in mixing rate induced by compressions. It is observed that the details of properties of shock turbulent mixing interaction strongly depend on the degree of mixing upstream from the compression. In particular, for a low mixing rate upstream of the pressure jump, the total stretch of surfaces is more controlled by curvature than by in-plane strain rate, whereas blob type injection leads to modifications of stretch induced by strain rate. Moreover, the strain rate becomes negative within the compression zone, and it rapidly relaxes to positive values downstream from the pressure jump, whereas the impact of weak shocks on the curvature of the field is sustained far downstream from the compression zone. Conclusions are drawn for further developments in modeling mixing.

Nomenclature

A_Y	= area of isosurfaces
D	= diffusion coefficient
\mathcal{F}_ψ	= generic mixing closure
$\mathcal{H}_{Y,u}$	= total stretch of the isosurfaces
K	= turbulent kinetic energy
M	= Mach number
n	= normal vector
P	= pressure
$\bar{P}(\psi; \underline{x}, t)$	= probability density function of Y
u	= velocity vector
\underline{x}	= position in space
Y	= mixture fraction
$\Gamma_{Y,u}$	= time evolution of Y
δ_s	= shock thickness
ϵ	= dissipation rate of K
ϵ_Y	= dissipation rate of Y''
θ_s	= total generation rate of surfaces
μ	= molecular viscosity
ρ	= density
$\bar{\Sigma}(\psi; \underline{x}, t)$	= surface density function of Y
τ_m	= mechanical time
τ_Y	= mixing time for Y
ϕ_s	= in-plane strain rate
ψ	= sample space variable of Y
Ω_Y	= diffusive budget
$ \nabla Y $	= magnitude of the gradient of Y

Subscripts

down	= downstream from the shock wave
up	= upstream from the shock wave

Superscripts

-	= Reynolds average
'	= Reynolds fluctuations, $() - \bar{ } $
$\bar{ } $	= Favre average, $\overline{\rho()} / \bar{\rho}$
"	= Favre fluctuations, $() - \bar{ } $

Introduction

THE interaction between compressible turbulence and strong or weak pressure discontinuities is a problem of interest for supersonic turbulent combustion devices. Usually fuel and oxidizer are initially separated and combustion occurs in nonpremixed regime. Because the amount of heat released by nonpremixed turbulent flames is highly sensitive to the rate of mixing between fuel and oxidizer, modifications of properties of scalar mixing have both theoretical and practical implications.

In this spirit, the interaction between a weak shock and a turbulent mixing zone is studied in the following by using direct numerical simulation (DNS) of the Navier–Stokes equations. The main objective of this work is to characterize modifications of turbulent mixing resulting from a compression. The mixing side of the problem is addressed through the concentration levels of a nonreactive species Y corresponding to the mixture fraction, widely utilized in the description of the internal properties of nonpremixed turbulent flames.¹ The properties of the mixing strongly depend on the behavior of the isoconcentration surfaces defined by the locations where $Y(\underline{x}, t) = \psi$ ($0 < \psi < 1$). These surfaces are convected and stretched by the turbulence of the flow.² To characterize the statistical properties of the iso- ψ surfaces, and therefore the properties of mixing, it is convenient to use as a guideline the transport equation for the surface density function (SDF) $\bar{\Sigma}(\psi; \underline{x}, t)$.^{3,4}

The SDF $\bar{\Sigma}(\psi; \underline{x}, t)$ of the scalar field $Y(\underline{x}, t)$ is the conditional mean of $|\nabla Y|$ for the value $\psi = Y$ weighted by $\bar{P}(\psi; \underline{x}, t)$, the

Presented as Paper 96-0517 at the AIAA 34th Aerospace Sciences Meeting, Reno, NV, Jan. 15–18, 1996; received Jan. 19, 1996; revision received Aug. 5, 1996; accepted for publication Aug. 18, 1996; also published in *AIAA Journal on Disc*, Volume 2, Number 1. Copyright © 1996 by the American Institute of Aeronautics and Astronautics, Inc. All rights reserved.

*Professor, Laboratoire de Mécanique des Fluides Numérique, URA-Centre National de la Recherche Scientifique-230, CORIA.

†Research Associate, Laboratoire de Mécanique des Fluides Numérique, URA-Centre National de la Recherche Scientifique-230, CORIA. Student Member AIAA.

probability density function (PDF) of Y . This definition leads to the statistical quantity $\bar{\Sigma}(\psi; \underline{x}, t)$ defined in one point and representing the mean density per unit of volume of the area of the iso- ψ surfaces.

It is possible to seek out two contributions to the evolution of these surfaces: the strain rate evaluated in the tangential plane to the iso-surface and the local curvature of the surface.⁵ Both in-plane strain rate and curvature control the total stretch of the surface. These two effects need to be accounted for in supersonic turbulent combustion modeling, and this can be done, for instance, when closing diffusion in PDF-based methods.^{6,7} Indeed, the development of turbulent combustion modeling for the supersonic regime including finite rate chemistry effects may be achieved by introducing PDFs.⁸ This modeling technique is attractive because a complex description of chemical processes can be included directly. The major stumbling block is then to propose a closure for the mixing (diffusive) part of the problem. Recent statistical models have been shown to provide encouraging results.^{9,10} It is interesting, however, to seek out the very basic properties that these models should reproduce when they are utilized for weakly nonisentropic flows. The mixing term entering the PDF transport equation is representative of strain and curvature of the isosurfaces and of their coupling with diffusion.³ The modeling of mixing terms is usually realized by introducing a mixing time scale⁶⁻¹⁰ entering a closed expression for the phenomena controlling diffusion. Furthermore, one generally formulates the hypothesis that mixing frequencies scale like the inverse of an eddy breakup scale based on the dissipation rate of the velocity field.

When comparing DNS data from both weak shock turbulence and weak shock vortices interactions, similitudes emerge between corresponding acoustic fields. From DNS results it is also possible to evaluate the impact of a weak compression on mixing time. In this context, it is observed that the frequency of scalar mixing is not proportional to the eddy breakup frequency evaluated from aerodynamical properties. Furthermore, a precise characterization of the effect of shock wave on mixing needs to account for the particular structure of the mixing zone upstream from the compression. In the case of a low degree of mixing, the mean value of the curvature of the scalar field $Y(\underline{x}, t)$ is modified by the presence of the compression and this effect is sustained far downstream from the weak shock. However, this behavior is different from the one observed for in-plane strain rate, which is localized within the weak shock zone. Moreover, it is found that for a segregated Y distribution upstream from the weak shock, the curvature is weakly modified across the compression. Finally, when the evolution for the overall interaction is considered, including the relaxation of the scalar field, the total stretch of isosurfaces is more controlled by curvature than by tangential strain rate in the case of a laminar injection, whereas dominant effects come from in-plane strain rate for a segregated distribution of mixture fraction. From these observations conclusions are drawn for mixing modeling to be utilized in PDF computations of nonpremixed turbulent combustion in supersonic regime.

Mixing and Statistical Description of Iso- ψ Surfaces

In this section basic quantities characterizing turbulent mixing and isoconcentration surfaces are presented. Diffusion at small scales of the turbulent motion as well as mixing are strongly related to the movement of the isoconcentration surfaces. It is possible to characterize these surfaces through pure geometrical considerations, and so far this point of view has generally been adopted. Along the same lines, a one-point statistical description of the surfaces is also of interest and can be achieved by introducing an SDF defined from $\bar{P}(\psi; \underline{x}, t)$ the PDF of Y . This last approach has been shown to be an effective tool to study the internal structure of turbulent premixed flames.⁴ Moreover, it yields to very simple mathematical relations to estimate, from DNS databases, geometrical properties of surfaces without having to introduce triangulation methods.⁴

The transport equation for the mixture fraction field Y may be written

$$\begin{aligned} \frac{\partial Y(\underline{x}, t)}{\partial t} &= -\mathbf{u} \cdot \nabla Y(\underline{x}, t) + \frac{1}{\rho} \{ \nabla \cdot [\rho D \nabla Y(\underline{x}, t)] \} \\ &= -\mathbf{u} \cdot \nabla Y(\underline{x}, t) + \Omega_Y(\underline{x}, t) = \Gamma_{Y,u} \end{aligned} \quad (1)$$

The transport equation for $\bar{P}(\psi; \underline{x}, t)$, the PDF of $Y(\underline{x}, t)$ may be written³

$$\frac{\partial \bar{P}(\psi; \underline{x}, t)}{\partial t} = -\frac{\partial}{\partial \psi} [(\Gamma_{Y,u}|Y = \psi) \bar{P}(\psi; \underline{x}, t)] \quad (2)$$

The density of isoconcentration surface per unit of volume may be defined through the PDF and the conditional mean value of the amplitude of the gradient in the form $\bar{\Sigma}(\psi; \underline{x}, t) = \bar{P}(\psi; \underline{x}, t) (|\nabla Y||Y = \psi)$; its corresponding transport equation may be written³

$$\begin{aligned} \frac{\partial \bar{\Sigma}(\psi; \underline{x}, t)}{\partial t} &= (\theta_s | \mathcal{A}_Y = \psi) \bar{\Sigma}(\psi; \underline{x}, t) \\ &\quad - \frac{\partial}{\partial \psi} [(\Gamma_{Y,u} | \mathcal{A}_Y = \psi) \bar{\Sigma}(\psi; \underline{x}, t)] \end{aligned} \quad (3)$$

where $(\theta_s | \mathcal{A}_Y = \psi) = \theta_s \bar{\Sigma}(\psi; \underline{x}, t) / \bar{\Sigma}(\psi; \underline{x}, t)$ is the surface mean of the total surface generation rate θ_s ,

$$\theta_s = -\mathbf{nn} : \nabla \mathbf{u} - \frac{\mathbf{n} \cdot \nabla \Omega_Y(\underline{x}, t) - \mathbf{nn} : \nabla [|\nabla Y(\underline{x}, t)|]}{|\nabla Y(\underline{x}, t)|}$$

where $\mathbf{n} = -\nabla Y(\underline{x}, t) / |\nabla Y(\underline{x}, t)|$ is the normal vector of the iso- ψ surfaces pointing toward small values of Y .

The various terms entering the transport equations for the PDF and the SDF may be understood as following: when describing the statistics of the field Y by $\bar{P}(\psi; \underline{x}, t)$, the conditional mean value of $\Gamma_{Y,u}$ modifies the shape and the amplitude of the PDF in composition space. Because the PDF is a conserved quantity,

$$\int_0^1 \bar{P}(\psi; \underline{x}, t) d\psi = 1$$

this term appears in the form of a flux. The surface mean of $\Gamma_{Y,u}$ plays a similar role and controls the transfer of area between the iso- ψ surfaces [Eq. (2)]. The θ_s term is a source that explains how surfaces are created or destroyed due to the strain rate in the tangential plane of the surface caused by the motion of the fluid and the dynamic change of Y defining the isosurface.

The amplitude of the diffusion term is one of the characteristics of mixing, and it is related to the level of curvature of the surface $\nabla \cdot \mathbf{n}$ through

$$\rho \Omega_Y = \mathbf{nn} : \nabla (\rho D \nabla Y) - \rho D |\nabla Y| \nabla \cdot \mathbf{n}$$

The crucial point in the PDF modeling technique is to estimate the conditional mean $(\Omega_Y | Y = \psi)$ controlling the flux of the PDF in sample space [see Eq. (2)] or to find an ad hoc procedure to mimic the effect of the term

$$\frac{\partial [(\Omega_Y | Y = \psi) \bar{P}(\psi; \underline{x}, t)]}{\partial \psi}$$

on PDF evolution.⁷ Most well-known mixing models⁷ may be cast in the generic form $\mathcal{F}_\psi / \tau_Y$. Moreover, for modeling convenience it is usual to separate the estimation of τ_Y from the one of \mathcal{F}_ψ . This is, for instance, the case when the flow is computed via a $\bar{K} - \bar{\epsilon}$ type description of the turbulence. These aspects of mixing modeling are discussed later for the particular case of flows including weak compression zones.

The area $\mathcal{A}_Y(\psi; t)$ of the isosurface $Y(\underline{x}, t) = \psi$ may be obtained from the SDF

$$\mathcal{A}_Y(\psi; t) = \iiint_V d\underline{x} \bar{\Sigma}(\psi; \underline{x}, t)$$

The surface stretch,⁵ defined as the relative time rate of change of the area, may then be expressed as

$$\frac{1}{\mathcal{A}_Y(\psi; t)} \frac{d\mathcal{A}_Y(\psi; t)}{dt} = \frac{1}{\mathcal{A}_Y(\psi; t)} \iint_{\mathcal{A}_Y(\psi; t)} dA(\underline{x}) \mathcal{H}_{Y,u}$$

where

$$\mathcal{H}_{Y,u} = \phi_s + (1/|\nabla Y|) \Omega_Y \nabla \cdot \mathbf{n} \quad (4)$$

and $\phi_s = -\mathbf{nn} : \nabla \mathbf{u} + \nabla \cdot \mathbf{u}$ is the in-plane strain rate.

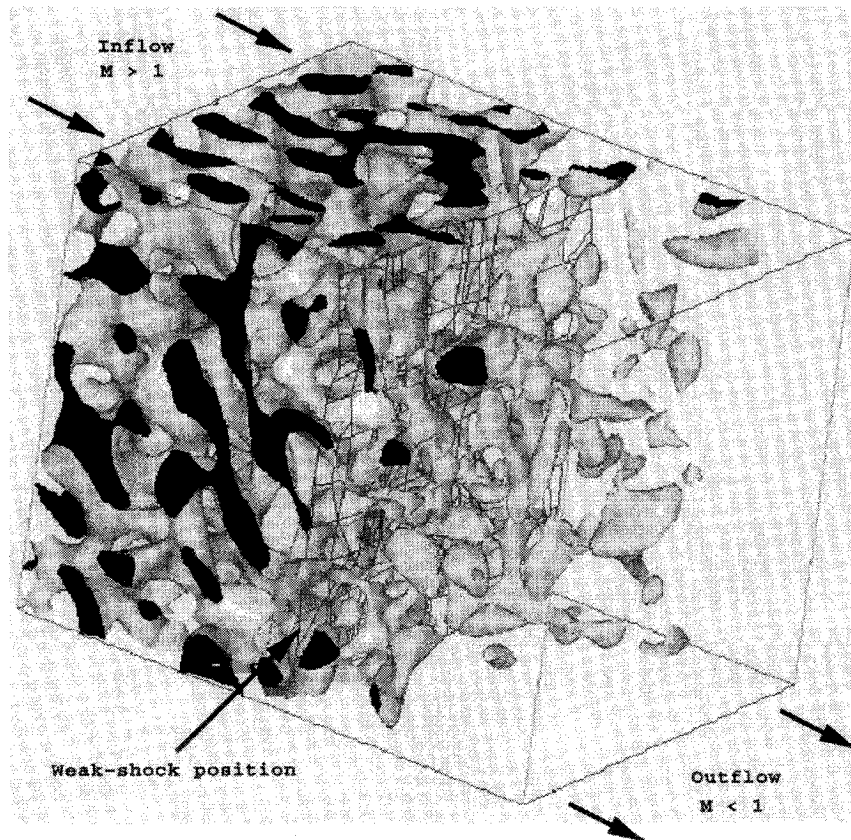


Fig. 1 Snapshot of the mixing zone interacting with a weak shock, blob type injection. Isoconcentration surfaces $\psi = 0.7$ are shown.

Numerical Procedure

The statistical properties of iso- ψ surfaces across a weak shock are extracted from three-dimensional simulations (129×65^2) performed by using a fully compressible DNS code.¹¹ It uses a sixth-order finite difference scheme¹² coupled with third-order time stepping and an appropriate boundary conditions treatment.¹³ The use of weak shock allows for solving the inner structure of the shock without adding any artificial treatment. A homogeneous turbulent velocity field interacts with the weak shock and a distribution of the nonreactive scalar field $Y(x, t)$ is convected toward the pressure jump (Fig. 1).

The turbulence is forced at the inlet of the computational domain,¹⁴ and two different distributions are considered for the scalar Y , injection of blobs, corresponding to a scalar field more or less segregated, and laminar injection (Fig. 2). These two types of injections correspond to different distribution of mixing zones upstream from the pressure jump. They have been chosen because in supersonic combustion systems shocks and weak compression may occur at different lengths from fuel injectors. A detailed description of the numerical procedure used for injecting the fluctuations of velocity may be found elsewhere.¹⁴ This methodology has been extended to the mixture fraction field. The injection of blobs is characterized by two parameters: $\bar{P}(\psi; x, t)$, the PDF of $Y(x, t)$, and the energetic spectrum of Y' . According to these quantities, and following an approach similar to the one used for the velocity field combined with a procedure to generate homogeneous scalar field,¹⁵ fluctuations are prescribed at inlet for the scalar $Y(x, t)$.

The Schmidt number of $Y(x, t)$ is set to unity. At the entrance of the computational domain, the turbulent Reynolds number based on the integral length scale is about 70, whereas the Reynolds number based on the initial Taylor microscale is about 50. The fluctuations Mach number is on the order of 0.1. The inlet Mach number M_{up} is set to 1.2, whereas values of pressure and density are those of the standard conditions. Results are made nondimensional by the inlet Mach number and by the thickness of the weak shock evaluated from an initial laminar condition¹¹ as $\delta_s = (P_{down} - P_{up}) / \max[\partial P(x) / \partial x]$. The inlet condition gives a

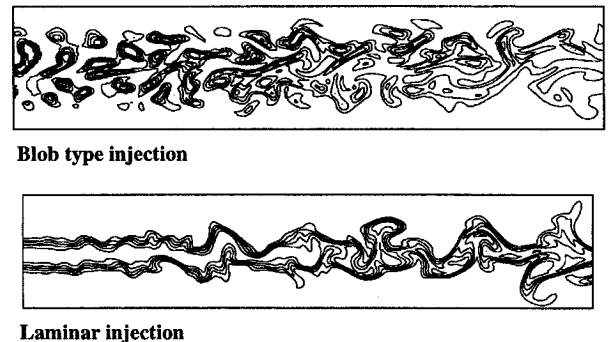


Fig. 2 Isolines of the mixture fraction field Y for the two types of injections (two-dimensional snapshots without shock).

ratio between the turbulent integral length scale of the turbulent flow and the characteristic weak shock thickness of about 20. The length of the computational domain corresponds to $100 \delta_s$, whereas the spanwise direction is about $80 \delta_s$. The numerical procedure,^{12,13} including the computation of the weak shock and details about grid generation and accuracy, have been carefully tested previously for two-dimensional¹¹ and three-dimensional¹⁴ problems.

Dynamics of Iso- ψ Surfaces Interacting with a Weak Shock

The aerodynamical properties of shock homogeneous turbulence interaction have been previously studied.¹⁴⁻¹⁶ For the present work, Fig. 3 displays two-dimensional snapshots of pressure field isocontours at six successive times. The distortion of the shock interface by the vorticity field is observed. In particular, secondary pressure discontinuities appear. These reflected shocks waves have been also found in single shock-vortex interaction.^{11,17,18} They result from the deformation of the weak shock by vorticity leading to a nonzero value of the component of the pressure gradient in the direction parallel to the shock (Fig. 4).

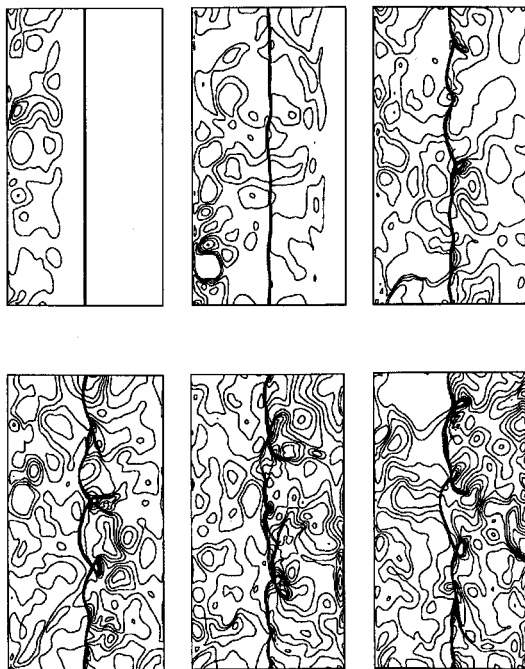


Fig. 3 Two-dimensional cuts of the pressure field for six successive times.

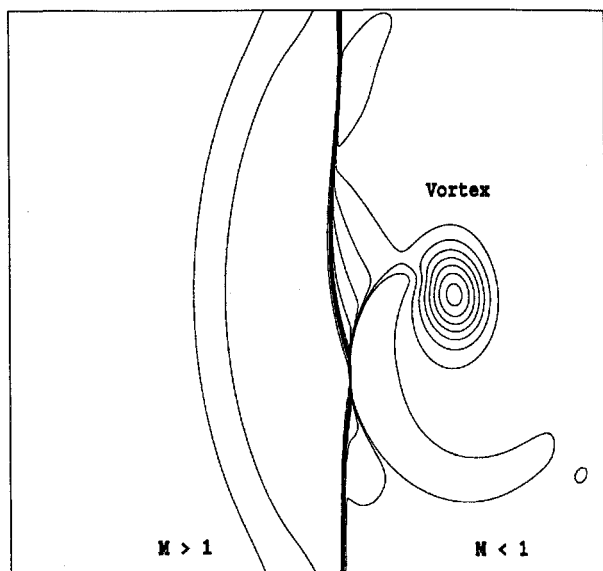


Fig. 4 Pressure field distribution in a shock single vortex interaction. Reflected shock waves resulting from the deformation of the shock are observed.¹¹

Mean values and surface means are computed in spanwise homogeneous directions (see Fig. 1), and then they are plotted vs the streamwise direction across the shock. The grid resolution chosen here for computing the statistic related to gradient has been previously tested for turbulent problems including weak discontinuities.⁴⁻¹⁹

To access the validity of simulations, known properties¹⁴ of shock turbulence interaction are recovered at first. In particular, an enhancement of the mean turbulent kinetic energy \bar{k} is observed at the shock interface, and this modification of the level of \bar{k} results from the amplification of the streamwise R_{11} component of the Reynolds stress tensor $R_{ij} = \rho u'_i u'_j / \bar{\rho}$.

The dissipation rate $\overline{\rho \epsilon}$ of the turbulent kinetic energy may be written

$$\overline{\rho \epsilon} = \overline{\rho \epsilon_s} + \overline{\rho \epsilon_c} = 2\mu \overline{\frac{\partial \omega'_i}{\partial x_j} \frac{\partial \omega'_j}{\partial x_i}} + \frac{4}{3}\mu \overline{\frac{\partial u'_i}{\partial x_i} \frac{\partial u'_i}{\partial x_i}} \quad (5)$$

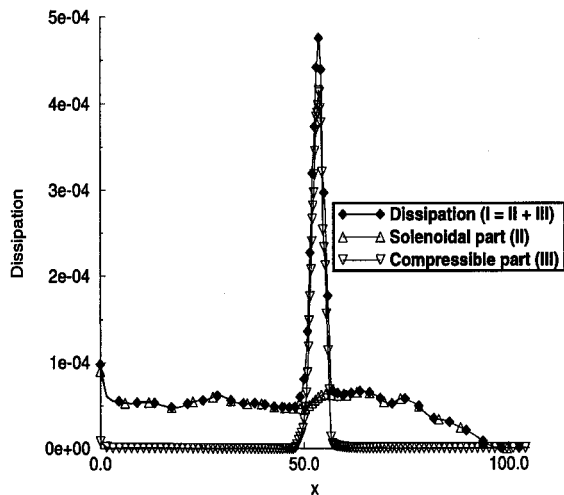


Fig. 5 Mean value across the shock of the dissipation rate of the turbulent kinetic energy I, solenoidal contribution II, and dilatation contribution III.

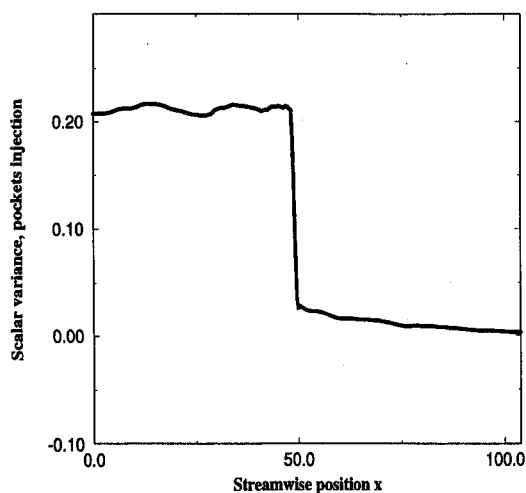


Fig. 6 Mean value of $\widetilde{Y''^2}$ across the shock for blob type injection.

where $\omega'_{i,j} = (\partial u'_i / \partial x_j - \partial u'_j / \partial x_i) / 2$. The first term, $\overline{\rho \epsilon_s}$, corresponds to the solenoidal part of the dissipation and it is not sensitive to the pressure discontinuity, whereas the compressible part, $\overline{\rho \epsilon_c}$, increases within the shock zone (Fig. 5).

The decay of the variance $\widetilde{Y''^2}$ computed for the blob type injection is an indicator of the efficiency of mixing. The streamwise evolution of $\widetilde{Y''^2}$ suggests that the shock strongly increases the scalar dissipation $\overline{\rho \epsilon_Y} = 2\rho D |\nabla Y''|^2$ (Fig. 6) and therefore mixing. Usually in modeling, the cascade mixing time $\tau_Y = \widetilde{Y''^2} / \overline{\rho \epsilon_Y}$ is estimated through $\bar{K} - \bar{\epsilon}$ modeling via $\tau_t = C_Y \tau_m$, where $\tau_m = \bar{K} / \bar{\epsilon}$ is a mechanical time and C_Y is taken as a constant. The streamwise distribution across the shock of the ratio τ_m / τ_Y shows that C_Y may be considered as constant in both isentropic flows upstream and downstream from the weak compression. In counterpart, C_Y is strongly modified within the weak shock zone (Fig. 7); this also is observed when $\bar{\epsilon}$ is estimated including its compressible part [Eq. (5)]. The modification of C_Y is very localized within the weak compression. As expected, the main modifications of properties of velocity occur where the slope of the mean pressure profile is maximum. A careful examination of the data shows that, across the mean pressure jump, the rapid decay of $\widetilde{Y''^2}$ is not observed at the same location.

Through the closed expression $\mathcal{F}_\psi / \tau_Y$ for diffusion, mixing models have direct implications on the topology of isoconcentration surfaces. In particular, they have to mimic the properties of ϕ_s and $\Omega_Y \nabla \cdot \mathbf{n} / |\nabla Y|$ controlling the stretch across the pressure jump. In nonpremixed turbulent flames, the in-plane strain rate ϕ_s , acting

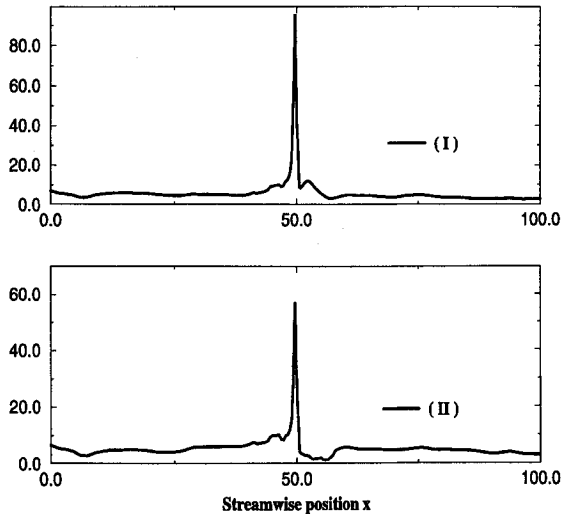


Fig. 7 Mean value of the ratio τ_m/τ_γ across the shock for blob type injection. In I, $\tau_m = \bar{K}/\bar{\epsilon}_s$; in II, $\tau_m = \bar{K}/\bar{\epsilon}$, where $\bar{\epsilon} = \bar{\epsilon}_s + \bar{\epsilon}_c$ [see Eq. (5)].

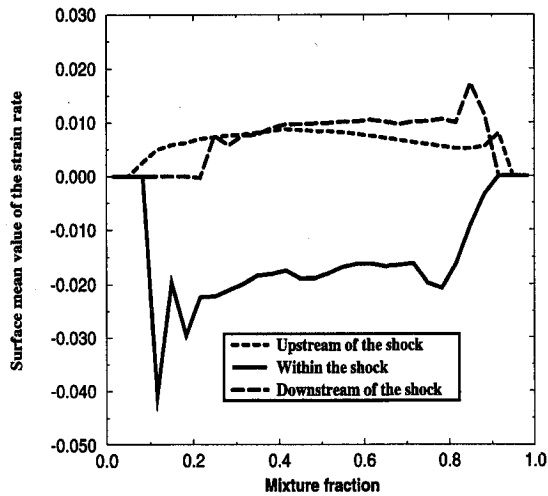


Fig. 8 Surface means of the in-plane strain rate $\phi_s = -nn : \nabla u + \nabla \cdot u$ at different streamwise locations for blob type injection.

along the iso- ψ surfaces, is correlated to the scalar dissipation rate $\bar{\epsilon}_\gamma$ that is an indicator of the local degree of mixing.¹⁹ Because of the compression across the pressure jump, it is expected for the in-plane strain rate to become negative within the weak shock interface. This modification of the strain rate is proportional to $\nabla \cdot u$ and should be found in the vicinity of the shock wave. This is confirmed by Fig. 8, in which surface means $(\phi_s|_{A_Y=\psi})$ are plotted at different locations within the streamwise direction for blob type injection. Because of compressibility effects, $(\phi_s|_{A_Y=\psi})$ becomes negative within the compression. Positive values of $(\phi_s|_{A_Y=\psi})$ are found, however, upstream and downstream of the weak shock. They correspond to an increase of the area of the iso- ψ surfaces. The streamwise evolution of the mean strain rate $\bar{\phi}_s$ evaluated in the homogeneous directions for the surface $\psi = 0.5$ shows that the compression is responsible for a local decrease of $\bar{\phi}_s$ (Fig. 9). As a consequence mixing is enhanced; indeed through the compression, the area of isoconcentration surfaces first decreases where $\bar{\phi}_s < 0$ [see Eq. (4)], and then it increases because of the relaxation of the mixture fraction field downstream from the compression (Fig. 10).

The mean value of the curvature of the scalar field $Y(\bar{x}, t)$ is also modified by the presence of the shock, and this effect is sustained far downstream of the shock (Fig. 11). For the blob type injection, the curvature is weakly affected by the shock (Fig. 11). This may be understood because, for one iso- ψ surface, increase or decrease of curvature provoked by the compression cancel out in the mean for

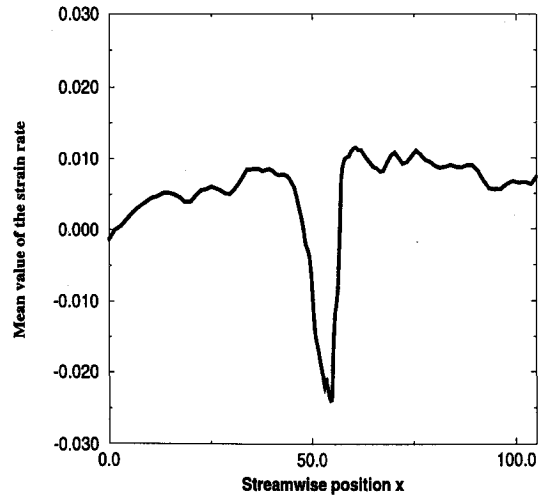


Fig. 9 Streamwise evolution of the mean strain rate $\bar{\phi}_s$ of the isosurface $\psi = 0.5$ for blob type injection.

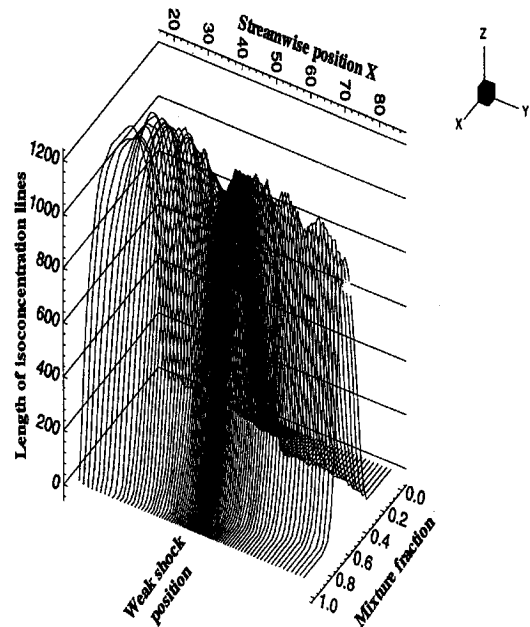


Fig. 10 Length of isoconcentration lines in homogeneous spanwise directions plotted for $0 < \psi < 1$ vs streamwise direction across the compression (blob type injection).

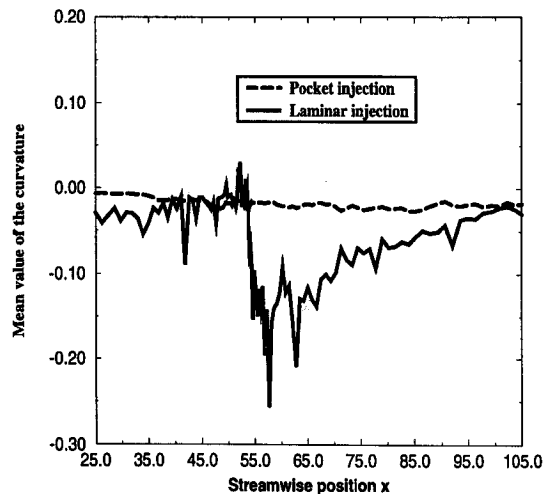


Fig. 11 Streamwise evolution of the mean level of curvature $\bar{\nabla} \cdot n$ of the isosurface $\psi = 0.5$ for the two types of injection.

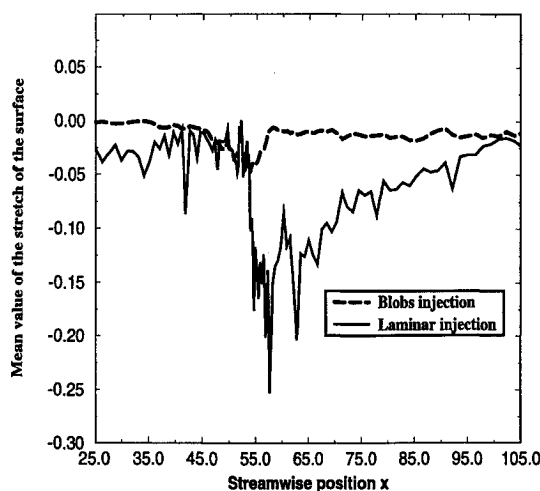


Fig. 12 Streamwise evolution of the mean stretch $\bar{\mathcal{H}}_{\gamma,u}$ of the isosurface $\psi = 0.5$ for the two types of injection.

segregated distributions. As a consequence, the mean streamwise evolution of the total stretch is essentially controlled by in-plane strain rate for the injection of blobs (Fig. 12). In counterpart for laminar injection, the total stretch of surfaces follows the relaxation of curvature induced effects (Fig. 12). Figure 12 suggests that, depending on the degree of mixing upstream of the shock, the impact of the pressure jump on the topological properties of isosurface may strongly differ.

From these DNS results one may deduce that a time scale based on shock properties is appropriate to characterize the relaxation of the in-plane strain rate downstream from the shock. The relaxation of curvature, however, is more linked to an eddy breakup time. Therefore, in-plane strain rate and curvature cannot be included simultaneously in a generic closure $\mathcal{F}_\gamma/\tau_\gamma$. These observations are of importance for the structure of nonunity Lewis number flames upon which curvature effects have a strong impact¹⁹ and may need to be included in PDF modeling.²⁰

Conclusion

PDF modeling may be of interest to compute flows in supersonic turbulent combustion devices. Then the turbulent mixing side of the problem needs to be carefully addressed. In this spirit, direct numerical simulations of shock turbulent mixing interaction have been carried out. The generated databases allow for studying the properties of both velocity and scalar field thoroughly.

From DNS, it is found that some of the features exhibited by a weak shock interacting with turbulence can be understood from basic shock vortices interactions. The hypothesis of a linear relationship between the mixing frequency and the inverse of a characteristic mixing time based on a turbulent cascade fails to describe the properties of the interaction between mixing and weak compression. This is observed essentially because compressibility effects have different impacts on both scalar dissipation rate and viscous dissipation of the velocity field. The behavior of isoconcentration surfaces is representative of the increase of mixing rate resulting from the compression. From the examination of these isoconcentration surfaces, basic properties that mixing models should reproduce emerge. Different types of scalar injection have been considered in the DNS. During the interaction, the modification of the in-plane strain rate is localized within the shock zone. In the case of laminar injection, the curvature of the scalar field is strongly sensitive to the presence of the pressure jump, and this effect is sustained far downstream of the shock. This is not the case for blob type injection,

where the total stretch is localized within the shock zone. This is observed because, for blob type injection, stretch is more controlled by strain rate than by curvature. This suggests that, across the shock, the mean behavior of the total stretch of isosurfaces, and therefore of mixing, depends on the upstream properties of the mixing zone. Moreover, it is required to treat separately in-plane strain rate and curvature effects in the modeling of mixing zones interacting with weak compressions.

Acknowledgment

This work has been funded by Direction de la Recherche et Etude technique (groupe 06) under Grant 93-2619A, "Simulation de l'interaction choc/turbulence."

References

- Bray, K. N. C., and Peters, N., "Laminar Flamelet in Turbulent Flame," *Turbulent Reacting Flows*, edited by P. A. Libby and F. A. Williams, Academic, London, 1994, pp. 63–113.
- Ottino, J. M., *The Kinematic of Mixing: Stretching, Chaos and Transport*, Cambridge Univ. Press, Cambridge, England, UK, 1989, Chap. 9.
- Vervisch, L., Bidaux, E., Bray, K. N. C., and Kollmann, W., "Surface Density Function in Premixed Turbulent Combustion Modeling, Similarities Between Probability Density Function and Flame Surface Approaches," *Physics of Fluids*, Vol. 7, No. 10, 1995, pp. 2496–2503.
- Vervisch, L., Kollmann, W., and Bray, K. N. C., "Dynamics of Iso-Concentration Surfaces in Turbulent Premixed Flames," Tenth Symposium on Turbulent Shear Flows, Paper 22-1, University Park, PA, Aug. 1995.
- Candel, S. M., and Poinot, T. J., "Flame Stretch and the Balance Equation for the Flame Area," *Combustion Science and Technology*, Vol. 70, 1990, pp. 1–15.
- Kollman, W., "The PDF Approach to Turbulent Flow," *Theoretic and Computational Fluid Dynamics*, Vol. 1, 1990, pp. 249–285.
- Dopazo, C., "Recent Developments in PDF Methods," *Turbulent Reacting Flows*, edited by P. A. Libby and F. A. Williams, Academic, London, 1994, pp. 375–474.
- Eiffler, P., and Kollman, W., "PDF Prediction of Supersonic Hydrogen Flame," AIAA Paper 93-04448, Jan. 1993.
- Fox, R., "Improved Fokker-Planck Model for the Joint Scalar, Scalar Gradient PDF," *Physics of Fluids*, Vol. 1, No. 6, 1994, pp. 334–348.
- Valiño, L., and Dopazo, C., "A Binomial Langevin Model for Turbulent Mixing," *Physics of Fluids*, Vol. 3, No. 12, 1991, pp. 3034–3037.
- Guichard, L., Vervisch, L., and Domingo, P., "Two-Dimensional Weak Shock-Vortex Interaction in a Mixing Zone," *AIAA Journal*, Vol. 33, No. 10, 1995, pp. 1797–1802.
- Lele, S. K., "Compact Finite Difference Schemes with Spectral Like Resolution," Center for Turbulence Research Rept., Stanford Univ., Stanford, CA, July 1990.
- Poinot, T., and Lele, S. K., "Boundary Conditions for Direct Simulations of Compressible Viscous Flows," *Journal of Computational Physics*, Vol. 101, No. 1, 1992, pp. 104–129.
- Lee, S., Lele, S. K., and Moin, P., "Direct Numerical Simulation of Isotropic Turbulence Interacting with a Weak Shock Wave," *Journal of Fluid Mechanics*, Vol. 251, 1993, pp. 533–562.
- Eswaran, V., and Pope, S. B., "Direct Numerical Simulation of the Turbulent Mixing of a Passive Scalar," *Physics of Fluids*, Vol. 31, No. 3, 1988, pp. 506–520.
- Hannappel, R., and Friedrich, R., "DNS of a $M = 2$ Shock Interacting with Isotropic Turbulence," *Direct and Large-Eddy Simulation I, Proceedings of the 1st ERCOFTAC Workshop on Direct and Large-Eddy Simulation*, edited by P. R. Voke, L. Kleiser, and J. P. Cholle, Kluwer Academic, Boston, 1994, pp. 359–373.
- Elzey, J., Heeneke, R., Picone J., and Oran, E., "The Interaction of a Shock with a Vortex: Shock Distortion and the Production of Acoustic Waves," *Physics of Fluids*, Vol. 7, No. 1, 1995, pp. 172–184.
- Ribner, H. S., "Cylindrical Sound Wave Generated by Shock-Vortex Interaction," *AIAA Journal*, Vol. 22, No. 11, 1985, pp. 1708–1725.
- Mahalingam, S., Chen, J. H., and Vervisch, L., "Finite-Rate Chemistry and Transient Effects in Direct Numerical Simulations of Turbulent Non-Premixed Flames," *Combustion and Flame*, Vol. 3, No. 203, 1995, pp. 285–297.
- Pope, S. B., "PDF Method for Turbulent Reacting Flows," *Combustion Science and Technology*, Vol. 11, 1985, pp. 119–195.